

8-2021

Spatiotemporal Methane Emission From Global Reservoirs

Matthew S. Johnson

Elaine Matthews

David Bastviken

Bridget Deemer

Jinyang Du

See next page for additional authors

Follow this and additional works at: https://digitalcommons.csumb.edu/aes_fac

This Article is brought to you for free and open access by the Department of Applied Environmental Science at Digital Commons @ CSUMB. It has been accepted for inclusion in AES Faculty Publications and Presentations by an authorized administrator of Digital Commons @ CSUMB. For more information, please contact digitalcommons@csumb.edu.

Authors

Matthew S. Johnson, Elaine Matthews, David Bastviken, Bridget Deemer, Jinyang Du, and Vanessa Genovese

JGR Biogeosciences

RESEARCH ARTICLE

10.1029/2021JG006305

Key Points:

- This study reports on a new global, gridded data set of spatiotemporal CH₄ emission from reservoirs
- Global reservoirs occupy an area of 297×10^3 km² and emit 10.1 Tg CH₄ yr⁻¹ via diffusion (1.2 Tg CH₄ yr⁻¹) and ebullition (8.9 Tg CH₄ yr⁻¹)
- This study addresses several key gaps and uncertainties existing in estimates of global reservoir CH₄ emission

Supporting Information:

Supporting Information may be found in the online version of this article.

Correspondence to:

M. S. Johnson,
matthew.s.johnson@nasa.gov

Citation:

Johnson, M. S., Matthews, E., Bastviken, D., Deemer, B., Du, J., & Genovese, V. (2021). Spatiotemporal methane emission from global reservoirs. *Journal of Geophysical Research: Biogeosciences*, 126, e2021JG006305. <https://doi.org/10.1029/2021JG006305>

Received 17 MAR 2021

Accepted 28 JUL 2021

Author Contributions:

Conceptualization: Matthew S. Johnson, Elaine Matthews, David Bastviken

Data curation: Matthew S. Johnson, Elaine Matthews, David Bastviken, Bridget Deemer, Jinyang Du, Vanessa Genovese




Formal analysis: Matthew S. Johnson, Jinyang Du, Vanessa Genovese

Funding acquisition: Elaine Matthews

Investigation: Matthew S. Johnson, Elaine Matthews, David Bastviken, Bridget Deemer, Jinyang Du, Vanessa Genovese

© 2021. American Geophysical Union. All rights reserved. This article has been contributed to by US Government employees and their work is in the public domain in the USA.

Spatiotemporal Methane Emission From Global Reservoirs

Matthew S. Johnson¹ , Elaine Matthews², David Bastviken³ , Bridget Deemer⁴ , Jinyang Du⁵, and Vanessa Genovese⁶

¹Earth Science Division, NASA Ames Research Center, Moffett Field, CA, USA, ²Bay Area Environmental Research Institute, NASA Ames Research Center, Moffett Field, CA, USA, ³Department of Thematic Studies–Environmental Change, Linköping University, Linköping, Sweden, ⁴Southwest Biological Science Center, U.S. Geological Survey, Flagstaff, AZ, USA, ⁵Numerical Terradynamic Simulation Group, University of Montana, Missoula, MT, USA, ⁶NASA Ames Research Center, California State University - Monterey Bay, Moffett Field, CA, USA

Abstract Inland aquatic systems, such as reservoirs, contribute substantially to global methane (CH₄) emissions; yet are among the most uncertain components of the total CH₄ budget. Reservoirs have received recent attention as they may generate high CH₄ fluxes. Improved quantification of these CH₄ fluxes, particularly their spatiotemporal distribution, is key to realistically incorporating them in CH₄ modeling and budget studies. Here we report on a new global, gridded (0.25° lat × 0.25° lon) study of reservoir CH₄ emissions, accounting for new knowledge regarding reservoir areal extent and distribution, and spatiotemporal emission patterns influenced by diurnal variability, temperature-dependent seasonality, satellite-derived freeze-thaw dynamics, and eco-climatic zone. The results of this new data set comprise daily CH₄ emissions throughout the full annual cycle and show that reservoirs cover 297×10^3 km² globally and emit 10.1 Tg CH₄ yr⁻¹ (1σ uncertainty range of 7.2–12.9 Tg CH₄ yr⁻¹) from diffusive (1.2 Tg CH₄ yr⁻¹) and ebullitive (8.9 Tg CH₄ yr⁻¹) emission pathways. This analysis of reservoir CH₄ emission addresses multiple gaps and uncertainties in previous studies and represents an important contribution to studies of the global CH₄ budget. The new data sets and methodologies from this study provide a framework to better understand and model the current and future role of reservoirs in the global CH₄ budget and to guide efforts to mitigate reservoir-related CH₄ emissions.

Plain Language Summary Methane (CH₄) is a greenhouse gas which contributes significantly to global warming and has atmospheric concentrations which have increased considerably in the last few decades, primarily due to human-induced emissions. Natural sources such as wetlands and inland aquatic systems (i.e., reservoirs, lakes, and rivers) contribute substantially to global emissions but these natural systems comprise the most uncertain components of the CH₄ budget. This study addresses multiple gaps and uncertainties associated with global CH₄ emissions from reservoirs and undertakes a spatial and temporal assessment of global reservoir emissions. The results from this study suggest that reservoirs occupy a global area about 300,000 km² (comparable to the size of the country of Italy) and emit 10.1 Tg CH₄ yr⁻¹. We identify data and methodological elements of previous estimates that indicate they may overestimate these emissions. This work provides a suite of global data sets, gridded at 0.25° × 0.25°, considering reservoir surface area, spatial distribution, eco-climatic system type, and the full annual cycle of daily CH₄ emissions.

1. Introduction

Methane (CH₄) is a potent greenhouse gas and its atmospheric concentration has increased significantly since the pre-industrial era and contributes to ~20% of present-day observed global warming (Ciais et al., 2013). Anthropogenic activities (e.g., fossil fuel use and production, waste disposal, and agriculture) emit around 350 Tg CH₄ yr⁻¹ (Saunio et al., 2016) and are assumed to be the primary contributors to increases in atmospheric CH₄ concentrations. Natural wetlands (which emit 100–200 Tg CH₄ yr⁻¹, Bloom et al., 2017; Melton et al., 2013) and inland aquatic systems (e.g., lakes, reservoirs, rivers) which together emit from 50 to >200 Tg CH₄ yr⁻¹ (Bastviken et al., 2004, 2011; Saunio et al., 2020; Rosentreter et al., 2021) are also significant emission sources of CH₄. These inland aquatic systems are currently considered the

Methodology: Matthew S. Johnson, Elaine Matthews, David Bastviken, Bridget Deemer, Jinyang Du, Vanessa Genovese

Supervision: Matthew S. Johnson, Elaine Matthews

most uncertain components of the global CH₄ budget (Kirschke et al., 2013; Rosentreter et al., 2021; Saunio et al., 2016, 2020; Thornton et al., 2016).

Reservoirs are created by the construction of dams that number in the millions world-wide (Lehner et al., 2011). These dam-reservoir systems are constructed for multiple purposes (e.g., hydroelectric power, flood control, water supply, recreation, and navigation) and are known to be sources of greenhouse gas emissions (Barros et al., 2011; Bastviken et al., 2004, 2011; Deemer et al., 2016; Harrison et al., 2021; St. Louis et al., 2000). The emission of CH₄ from reservoirs occurs via multiple pathways such as diffusion, ebullition, plant-mediated transport, degassing from turbines and spillways, and water drawdown events (Deemer et al., 2016; Harrison et al., 2021) and is controlled by numerous physiochemical properties of individual reservoirs (Prairie et al., 2017).

Previous global estimates of reservoir CH₄ emission are scarce and variable, ranging from 18 to 70 Tg CH₄ yr⁻¹ (i.e., from <3 to >10% of the global CH₄ budget (Deemer et al., 2016; St. Louis et al., 2000). These studies often rely on simple assumptions about regional and global reservoir areas and length of emission seasons, and employed different subsets of flux measurements to estimate global emissions. Most importantly, none of the existing global estimates provide CH₄ emissions which are both spatially and temporally explicit. While the recent study by Harrison et al. (2021) incorporated temporal variability into their estimates of annual-scale emission, gridded estimates of sub-annual CH₄ emission are not provided. This study provides gridded estimates of daily CH₄ emission from reservoirs which is a critical requirement for use in bottom-up biogeochemical and top-down atmospheric CH₄ emission modeling.

Here we use measurements of CH₄ emission from 161 globally distributed reservoir systems in boreal, temperate, and tropical/subtropical regions, compiled by Deemer et al. (2016) to develop a gridded data-driven model of reservoir CH₄ emissions that is also temporally explicit. This flux measurement synthesis includes data for diffusive and ebullitive flux pathways as well as additional emission processes (e.g., degassing at dams, drawdown marshes, and downstream rivers influenced by turbines and spillways). Most of the observations reflect diffusive and ebullitive fluxes which have been the focus of previous studies as well as the one presented here. Confident estimates of reservoir fluxes associated with these alternative emission pathways are problematic due to minimal data and untested methodologies. Therefore, this study focuses on the main emission pathways of diffusion and ebullition.

The data in Deemer et al. (2016) illustrate the large spatial variability in diffusive and ebullitive fluxes among reservoirs. This variability is the result of heterogeneity in reservoir physiochemical characteristics (e.g., surface area, depth, water/sediment composition, and meteorological conditions), measurement techniques (e.g., boundary layer methods, floating chambers, eddy covariance and acoustic methods, and bubble traps), and field measurement designs (e.g., time of year and day when measurements are acquired, frequency, and duration of measurement campaigns).

This study focuses on the development of new data sets and a data-driven model to address the key gaps in current reservoir CH₄ emission estimates with the goal of reducing uncertainties in global emissions associated with: (a) area and distribution of reservoirs; (b) eco-climatic classification (boreal, temperate, and tropical/subtropical) and integration of fundamental influences of regional climate and water/soil characteristics; (c) time of day of measurements that addresses recently observed diel variability in emissions; (d) emission seasonality based on both time of the year of sampling and temperature-dependence of emissions; and (e) emission seasonality defined by satellite observations of the timing and duration of ice-cover and freeze-thaw dynamics. This study was undertaken in the context of better understanding the global CH₄ cycle and focuses specifically on the diffusive and ebullitive emissions of CH₄ from the water surface of existing reservoirs, and albeit important, does not attempt to quantify the net carbon impact of reservoir creation. We report on a novel suite of global gridded data sets representing reservoir area and distribution, reservoir eco-climatic type, and daily CH₄ fluxes throughout the full annual cycle accounting for emission season length.

2. Data and Methods

All data sets employed and produced in this study are at 0.25° × 0.25° (latitude × longitude) spatial resolution.

2.1. Reservoir Surface Area, Distribution, and Eco-Climatic Type

Reservoir areal extents have received less attention than those of wetlands and lakes; however, several data sets of reservoir area and abundance have been published. These data are typically in tabular, or in polygon shape files or vector formats—which are spatial but not in a standard gridded format—and thus are not directly adaptable for use in global bottom-up biogeochemical or top-down inverse models of CH₄ emission. These reservoir area data sets include the Global Lakes and Wetlands Database (GLWD) (Lehner & Döll, 2004) (polygon shape file); Global Reservoirs and Dams (GRanD) (Lehner et al., 2011) (polygon shape file); HydroLAKES (Messenger et al., 2016) (polygon shape file); GLObal geOreferenced Database of Dams (GOOD2) (Mulligan et al., 2009) (tabular, location only, no areas); and the International Commission on Large Dams (ICOLD, 1988, 1998, 2006) (tabular, location, many lacking area). We note that Lehner and Döll (2004), Lehner et al. (2011), Messenger et al. (2016) (HydroLAKES), and GRanD comprise essentially the same data on ~6,800 large reservoirs with storage capacity ≥ 0.1 km³.

Global reservoir areas and locations for this study were extracted from HydroLAKES (Messenger et al., 2016) using the GRanD v1.1 database (Lehner et al., 2011) for the locations of ~6,800 large reservoirs. We included only reservoirs from Lehner et al. (2011) and excluded regulated lakes (which account for ~40% of the total reservoir and regulated lake area in GRanD). This was done because these systems often function more like lakes than reservoirs. Moreover, the CH₄ flux compilation applied in this study (see Section 2.2.1) contains data only from aquatic systems identified specifically as reservoirs. Lastly, since regulated lakes in Lehner et al. (2011) could be considered reservoirs or lakes, excluding them minimizes uncertainty associated with the reservoir CH₄ source and avoids overestimating CH₄ emission from reservoirs.

We augmented the GRanD/HydroLAKES data with ~35,000 dams from GOOD2 v1 (Mulligan et al., 2009) which reports locations but not reservoir area. We added surface areas for these small reservoirs based on coincident water bodies from the European Space Agency (ESA) Climate Change Initiative Inland-Water (CCI-IW) remote-sensing data (Lamarche et al., 2017). Combining the GRanD and GOOD2 data resulted in a total global reservoir area of 297×10^3 km² for ~42,000 reservoirs.

Reservoirs were classified into eco-climatic regions (i.e., boreal, temperate, and tropical/subtropical) to facilitate identifying them with region-specific CH₄ fluxes calculated from a compilation of reservoir CH₄ flux measurements (Section 2.2.1). Eco-climatic regions were defined using annually averaged soil temperature as follows: boreal/arctic reservoirs are those with annually averaged soil temperature $\leq 5^\circ\text{C}$ following Petrescu et al. (2010); annual mean soil temperatures $>5^\circ\text{C}$ and $\leq 20^\circ\text{C}$ denote temperate reservoirs, and soil temperatures $>20^\circ\text{C}$ define tropical/subtropical reservoirs. To prescribe soil temperatures, we calculated a multi-year annually averaged (for 2002–2015) modeled soil temperature data set (0–10 cm depth) from Modern-Era Retrospective analysis for Research and Applications, Version 2 (MERRA-2, Gelaro et al., 2017). This multi-year-averaged MERRA-2 soil temperature data set was used to avoid anomalous years.

2.2. Reservoir CH₄ Fluxes

This section describes the reservoir CH₄ flux measurement compilation, and how it was augmented, processed, and applied in this study. Additionally, we describe the data-driven model developed to correct flux observations and emission estimates for diurnal emission patterns and seasonal temperature-dependence, and the use of satellite-derived observations of freeze-thaw dynamics. A visualization of the steps taken to derive mean 24-h-averaged, diurnally and seasonally corrected, reservoir CH₄ emission rates is presented in Figure S1.

2.2.1. Daily CH₄ Emissions

The flux compilation derived here originated with data for the 161 globally distributed reservoir systems reported by Deemer et al. (2016). The number of sites used in Deemer et al. (2016) that had separated diffusive

and ebullitive fluxes was 196 (143 diffusion and 53 ebullition) with an additional 75 for total CH₄ emissions (no separation between diffusion and ebullition). We reassessed and augmented this data set as follows. For all measurement sites, original references in Deemer et al. (2016) were reviewed to extract information on measurement technique (e.g., boundary layer methods, floating chambers, eddy covariance and acoustic methods, and bubble traps), water and air temperature contemporaneous with flux measurements, time of day (daytime only or 24-h measurements) and time of year (month of observation). Individual measurements used to derive the averaged emission rates in Deemer et al. (2016) were expanded in our measurement compilation. The data added to our synthesis resulted in 467 individual measurements (189 diffusion; 98 ebullition; 180 total — all shown in Data Set S1). Subsequently, data were filtered to remove the small number of measurements reflecting turbine-influenced and downstream emissions, as well as those derived from indirect measurements (i.e., acoustic methods). Lastly, only measurements with information about time of day and year, and those distinguishing between diffusive and ebullitive fluxes, were used in this study. After our literature reassessment and filtering, 198 (127 diffusion; 71 ebullition) flux measurements were included in the present study. Boreal, temperate, and tropical/subtropical reservoirs were associated with daily emission rates (diffusive + ebullitive) calculated from this measurement compilation using the latitude and longitude of each measurement and the gridded soil-temperature data described in Section 2.1.

Sieczko et al. (2020) demonstrated that CH₄ fluxes from lakes during daytime hours are larger than those in the early morning and nighttime. To date, daytime measurements were typically used to represent daily averages, thus likely overestimating CH₄ emissions. Most measurements in our synthesis were made during the daytime hours. To correct for diurnal fluctuations in CH₄ emissions from reservoirs, we relied on information on the time of day for each measurement in our flux compilation. To derive true 24-h mean CH₄ flux rates (assuming that the diel variability of reservoir CH₄ fluxes is the same as lakes), the diurnal scaling factor of Sieczko et al. (2020) was applied to daytime observations. Specifically, daytime-only measurements (i.e., between 7:00 and 20:00 local time) were multiplied by 0.7 and measurements made over 24-h intervals were used as reported. The finding of higher daytime aquatic CH₄ fluxes is compatible with mechanistic explanations related with hydrodynamics (Sieczko et al., 2020) and the few individual studies reporting higher nighttime fluxes compared to daytime fluxes were typically based on eddy covariance methods or models, for which it is more challenging to isolate explanations (e.g., Podgrajsek et al., 2014). However, if nighttime fluxes are in fact higher in some reservoirs during the periods of reported measurements, our 24-h correction would result in a conservative estimate of reservoir CH₄ emissions.

2.2.2. Temperature-Dependent CH₄ Flux Seasonality

The majority of measurements in our synthesis were taken during the late spring to early fall. It is commonplace to use these measurements as daily averaged fluxes throughout the year. However, given that lake and reservoir CH₄ emission rates are positively correlated with air and water temperature (Aben et al., 2017; Jansen et al., 2020), this method likely leads to overestimates of lake and reservoir CH₄ emissions. We addressed this bias by calculating the seasonal distribution of CH₄ emissions for each measurement using methods similar to Prairie et al. (2017). To achieve this, we used derived relationships between air temperature and ebullition and diffusive fluxes considered separately. These temperature-flux relationships were used to derive a scaling factor expressing relative fluxes for all months based on the seasonal temperature cycle at the location of each measured reservoir—that is, by setting total yearly ice-free ebullition and diffusive fluxes to one (representing 100%) and solving for the fraction of this flux emitted each month given local monthly mean temperatures and the temperature-flux relationships. This allowed us to calculate monthly mean daily fluxes and total open-water fluxes from each sampled system corrected to a 24-h cycle to represent temperature-based flux seasonality. This strategy using monthly averages to derive temperature-modulated seasonality was chosen because information on the sampling month was more abundant in the literature than information about temperature during individual flux measurements.

Long-term mean air temperatures are assumed to be approximately similar to surface-water temperatures. The air temperature for each measurement site in the compilation was extracted from monthly averaged MERRA-2 two-meter air temperature data. A multi-year-averaged (for 2002–2015) MERRA-2 two-meter air temperature data set was calculated to reflect average conditions and avoid anomalous years.

We derived relationships between air temperature and ebullitive emission using a modified Arrhenius equation used to demonstrate a strong relationship between air temperature and ebullitive CH₄ fluxes from ponds in multiple eco-climatic zones (Aben et al., 2017), and regression fits for diffusive (Natchimuthu et al., 2016) emissions. To derive the temperature dependence of ebullitive fluxes we apply the modified Arrhenius equation shown in Equation 1

$$E_B = E_{20} \times \theta_s^{(T-20)} \quad (1)$$

where E_B is the ebullitive emission rate (mg CH₄ m⁻² day⁻¹), E_{20} is the ebullition emission rate at 20°C, θ_s is the system temperature coefficient, and T is the surface air temperature (°C). For this study, we applied an E_{20} value of 100 mg CH₄ m⁻² day⁻¹ and θ_s of 1.1 which is an average system temperature coefficient for air temperature of subtropical and temperate ponds from Aben et al. (2017). Our air temperature and ebullition flux fit is insensitive to E_{20} because this variable in Equation 1 only controls the magnitude of E_B while the correction applied here to derive monthly emission rates is the monthly fractional contribution of ebullitive emissions. Monthly E_B values are thus constrained by applying the actual measurement flux to the curve of fractional monthly emission factors.

A similar method was applied for diffusive fluxes using the regression fit of air temperature and diffusive CH₄ emissions from Natchimuthu et al. (2016) using Equation 2

$$E_D = 0.023e^{0.124T} \quad (2)$$

where E_D is the diffusive emission rate (mg CH₄ m⁻² day⁻¹) and T is the surface air temperature (°C). The fits in Equation 2 are derived from averages of regression fits from measurements of two Scandinavian lakes (one smaller and shallower lake [Skottenesjon] and a larger deeper water body [Erssjon]) in a hydrologically managed catchment with long-term measurements of air temperature and diffusive CH₄ fluxes (Natchimuthu et al., 2016). The regression fit for air temperature influence on diffusive emission rates from Natchimuthu et al. (2016) demonstrates moderate predictability with correlation coefficient (R^2) values between 0.35 and 0.46. Still, this relationship in Equation 2 was selected as one of the best available options for the following reasons: (a) Natchimuthu et al. (2016) is one of very few studies that relies on multiple years of continuous measurements of diffusive fluxes for different lakes; (b) the relationship was derived with data from a small number of well-understood aquatic systems instead of being based on fewer scattered measurements in multiple systems which are heavily confounded by inter-system variability and thereby less likely to reflect local temperature effects; (c) the specific temperature influence on underlying biochemical processes related to CH₄ formation appears to be relatively similar among systems (Marotta et al., 2014; Yvon-Durocher et al., 2014); and (d) we found no equally well-supported temperature-diffusive flux relationships for more globally representative reservoirs. We do note that various fits between diffusive CH₄ fluxes and air and water temperature have been derived (e.g., Yvon-Durocher et al., 2014; Marotta et al., 2014; Jansen et al., 2020), and using these different fits could impact the seasonality of reservoir diffusive emissions reported here. It should be noted that the application of Equations 1 and 2 assumes that the temperature-dependence of ebullitive and diffusive emissions in reservoirs is the same as that in lakes.

2.2.3. Reservoir Freeze-Thaw-Dependent Seasonality

In addition to the temperature-dependent emission seasonality derived with Equations 1 and 2, ice-cover-related CH₄ emission seasonality was incorporated using satellite observations of ice-cover and freeze-thaw dynamics as described in Matthews et al. (2020). We used two published satellite data products: lake-ice phenology (Du & Kimball, 2018) and landscape freeze/thaw dynamics (Kim et al., 2017a, 2017b; version 4 (FTv04)) to define reservoir emission seasons.

Lake-ice phenology (2002–2015) information was derived from the time series of 37 GHz brightness temperature (T_b) data of the Advanced Microwave Scanning Radiometer for EOS and Advanced Microwave Scanning Radiometer 2 (AMSR-E/2) sensors using a moving t -test algorithm (described in Du et al., 2017; Du & Kimball, 2018). Satellite microwave observations are largely unhindered by cloud and polar darkness, which allows for daily measurements of global lake-ice conditions. The resulting lake-ice phenology record shows 95% temporal agreement with available ground-based observations from the Global Lake and River Ice Phenology Database (Du et al., 2017). The phenology data were used for Northern Hemisphere reservoirs with surface areas ≥50 km² to minimize potential land contamination in the AMSR-E/2 observations.

Daily landscape freeze-thaw dynamics from 2003 to 2015 (described in Kim et al., 2017a, 2017b; version 4 (FTv04)) were used in this study for reservoirs lacking data on lake-ice phenology. Freeze-thaw signals were determined from calibrated 37 GHz Tb data of the Special Sensor Microwave Imager (SSM/I), and SSM/I Sounder (SSMIS) using a seasonal thresholding scheme with classification accuracies higher than 84% relative to global weather station measurements.

These two satellite data sets were employed to develop a year of global daily data describing the timing and duration of the ice-free periods which define the seasonality of reservoir CH₄ emissions. A thaw season identification algorithm was applied to each 5 km pixel of the satellite data sets. To identify thaw season onset and duration, a 21-day moving window was applied to the annual time series to ensure a robust detection of ice phenology similar to previous studies (Du et al., 2017; Zhang et al., 2011). A 21-day window was defined as “thawed” if at least 15 of the 21 days during the window were classified as thawed. The thaw onset was defined as the middle of the first 21-day window during the thaw season, and similarly the end date of thaw season was determined as the middle of the last 21-day thaw window. The pixel-level freeze and thaw dates were then averaged to the 0.25° × 0.25° spatial resolution used in this study.

2.2.4. Integration of Temporal Variability

Mean 24-h-averaged ebullitive and diffusive emission rates, which varied by month, were calculated for each site in the data synthesis. The flux sites were then classified into eco-climatic domains using the same soil-temperature criteria as described in Section 2.1. Mean diffusive and ebullitive emission rates were then calculated for boreal, temperate, and tropical/subtropical reservoirs (see Figure S2). Monthly mean daily ebullitive and diffusive emission rates were then summed to calculate total daily emission rates which were applied throughout the ice-free season to arrive at a total annual CH₄ emission.

The daily fluxes and total emission explicitly account for diel, seasonal, ice-cover, and eco-climatic variability, thus reducing uncertainties introduced by using both constant emission season lengths, constant daily fluxes, and simple assumptions for reservoir freeze-thaw dynamics as done in past studies (e.g., Barros et al., 2011; Bastviken et al., 2011; Deemer et al., 2016; Harrison et al., 2021; St. Louis et al., 2000).

2.2.5. Other Emission Pathways

Our reservoir CH₄ emission estimate includes the main flux pathways of diffusion and ebullition, but several other pathways have been recognized. For instance, CH₄ can accumulate under surface ice and be rapidly released at spring ice melt (e.g., Denfeld et al., 2018; Duchemin et al., 2006; Jammet et al., 2015; Jansen et al., 2019; Karlsson et al., 2013; Phelps et al., 1998). CH₄ pulses can also occur upon water-column mixing if anoxic portions of the water column have accumulated CH₄ during stratification periods (Schubert et al., 2012). While the latter process is recognized as potentially important in lakes, it is less well understood in reservoirs where mixing or stratification dynamics are more complex and influenced by local reservoir management (e.g., Bastviken et al., 2004; Demarty et al., 2011). Additional fluxes, such as degassing in turbines and emissions from downstream rivers, are also known to occur in reservoirs (Deemer et al., 2016) and Harrison et al. (2021) recently reported on global degassing emissions. We did not include these emission pathways because data specific to these alternative flux pathways are currently limited. Consequently, our study may underestimate total CH₄ emissions from reservoirs.

3. Results and Discussion

3.1. Reservoir Surface Area

Global reservoir surface area is estimated to be 296.6×10^3 km² (see Table 1) and Figure 1a shows the reservoir area density (percent area of grids). Reservoirs are concentrated in the temperate regions of North America and Europe and tropical/subtropical regions of South America and Asia which are locations with large human populations. Latitudinal patterns of reservoir areas (see Figure 2) show a broad distribution across temperate and tropical/subtropical latitude zones, and a boreal peak between 50° and 55°N which is due to the small number of very large reservoirs in Canada and Eurasia (e.g., Smallwood Reservoir, Lake Winnipeg, Irkutsk Reservoir, Kuybyshev Reservoir).

Table 1
Reservoir Eco-Climatic Class, Area, Number of Observations, Mean Emission Season Length, Mean Daily Emission-Season Flux Rate, and Total Annual CH₄ Emission (Diffusion + Ebullition)

Eco-climatic type	Area (10 ³ km ²)	Obs. #	Mean emission season (days)	Mean emission season CH ₄ flux (mg m ⁻² day ⁻¹)	Annual CH ₄ emission (Tg yr ⁻¹)
Boreal	65.5	53	167	39.1	0.4
Temperate	123.9	81	282	140.9	4.9
Tropical/subtropical	107.2	64	363	121.4	4.8
Total	296.6	198			10.1

Figures 1 and 2 show that, aside from the large peak in reservoir surface area in the boreal region, reservoirs are primarily present in the temperate and tropical/subtropical latitudes. On a global scale, boreal reservoirs, which are typically present >50°N, contribute ~22% ($65.5 \times 10^3 \text{ km}^2$) to the global reservoir area (see Table 1). Reservoirs classified as temperate make up ~42% ($123.9 \times 10^3 \text{ km}^2$) of the total area and are primarily located between 30° and 50°N. Finally, tropical/subtropical reservoirs account for ~36% ($107.2 \times 10^3 \text{ km}^2$) of total reservoir area and are primarily located between 20°S and 25°N.

Our global reservoir area is estimated to be $296.6 \times 10^3 \text{ km}^2$ (see Table 1) and is lower than several past estimates (Bastviken et al., 2011; Downing et al., 2006; St. Louis et al., 2000) and similar to others (Deemer et al., 2016; Harrison et al., 2021; Lehner & Doll, 2004; Lehner et al., 2011; Messenger et al., 2016). Similarities are expected because several of these studies rely on the same, or closely related, data on reservoir areas (see Table 2), and exclude regulated lakes as discussed above.

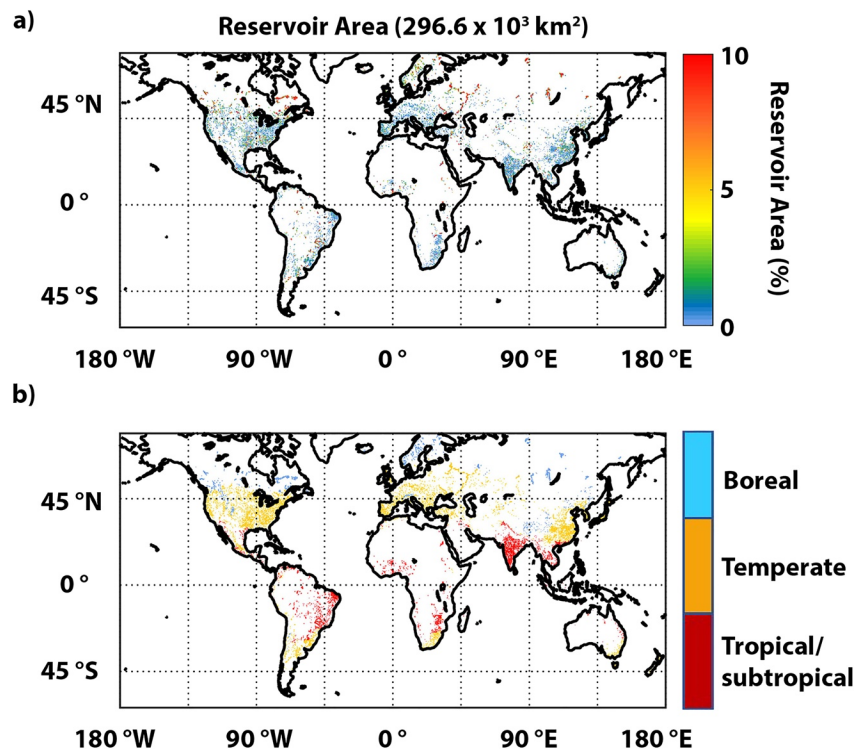


Figure 1. (a) Reservoir area density (percent area of grid) and (b) reservoir eco-climatic zone classification. White indicates areas with no reservoirs.

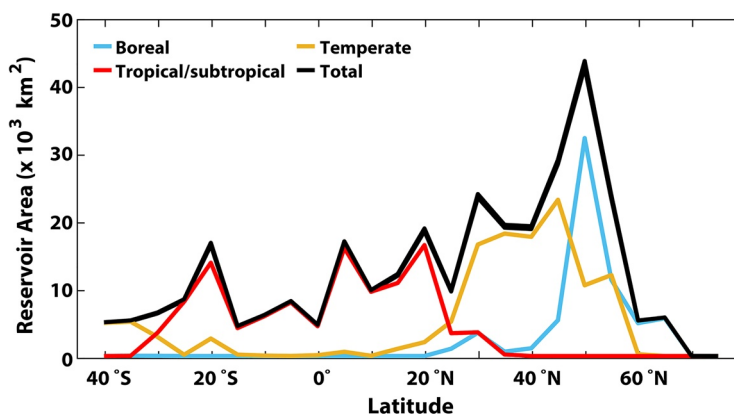


Figure 2. Zonal sums (5° latitudes, x-axis label represents the southern limit of zones) of reservoir surface areas by eco-climatic types. Note that eco-climatic zones are defined by annual mean soil temperatures and not latitudes.

3.2. Reservoir CH₄ Emission

3.2.1. Daily CH₄ fluxes

The emission-season-mean daily CH₄ fluxes (daily mean fluxes only during the thaw season) for eco-climatic reservoir types are shown in Table 1. When comparing the emission-season-mean daily CH₄ fluxes it can be seen that boreal reservoirs typically have the lowest emission rates ($39.1 \text{ mg CH}_4 \text{ m}^{-2} \text{ day}^{-1}$), with temperate ($140.9 \text{ mg CH}_4 \text{ m}^{-2} \text{ day}^{-1}$) and tropical/subtropical ($121.4 \text{ mg CH}_4 \text{ m}^{-2} \text{ day}^{-1}$) systems displaying higher emission rates. The current sentiment is that tropical aquatic systems have higher areal CH₄ emission rates compared to temperate lakes and reservoirs; however, the compilation of reservoir fluxes used in this study does not reflect this. This agrees with Deemer et al. (2016) which showed that CH₄ emission rates from temperate and tropical/subtropical reservoirs are statistically consistent.

3.2.2. Global CH₄ Emission

Reservoir surface areas in our data set are largest in the temperate and tropical/subtropical regions which drives the spatial distribution of CH₄ emissions from these inland aquatic systems (see Figure 3). Applying daily time- and temperature-corrected eco-climatic emission rates, remote-sensing-derived emission season lengths (see Table 1, Figure 3), and spatially distributed eco-climatic reservoir classifications (see Figure 1), we estimate a global reservoir CH₄ emission of $10.1 \text{ Tg CH}_4 \text{ yr}^{-1}$ ($1.2 \text{ Tg CH}_4 \text{ yr}^{-1}$ via diffusion, $8.9 \text{ Tg CH}_4 \text{ yr}^{-1}$ via ebullition). Considering the coefficient of variation in the time- and temperature-corrected diffusive and ebullitive emission measurements, we calculated a 1σ uncertainty range of $7.2\text{--}12.9 \text{ Tg CH}_4 \text{ yr}^{-1}$. Figure 4 shows zonal sums of annual reservoir CH₄ emissions. The high density of reservoirs in temperate and tropical/subtropical regions, and their long emission seasons, combine to produce a broad band of substantial tropical/subtropical reservoir emissions distributed between 20°S and 25°N while emissions in the temperate regions are relatively evenly spread between 30° and 50°N . The peak in area in boreal regions (Figure 2), moderated by the short emission season, results in very low emissions equal to only a few percent of the global total.

3.2.3. Reservoir Eco-Climatic Zone CH₄ Emission

Boreal reservoirs are primarily located in Canada, northern Europe, and Siberia. In the high latitude regions $>50^\circ\text{N}$, these boreal reservoirs contribute a small amount to global CH₄ emission. Due to the small number of reservoirs, short emission seasons, and low air/water temperatures in high latitudes, boreal reservoirs are characterized by low ebullitive and diffusion fluxes and contribute around 4% ($0.4 \text{ Tg CH}_4 \text{ yr}^{-1}$) to global emissions (see Table 1). Temperate reservoirs, concentrated in populated regions of the United States, Europe, and China, contribute around 48% ($4.9 \text{ Tg CH}_4 \text{ yr}^{-1}$) to global reservoir emissions. Finally, 48% ($4.8 \text{ Tg CH}_4 \text{ yr}^{-1}$) of total emissions come from tropical/subtropical reservoirs which are mostly located in Brazil and Argentina in South America, central and southern Africa, India, and southern China.

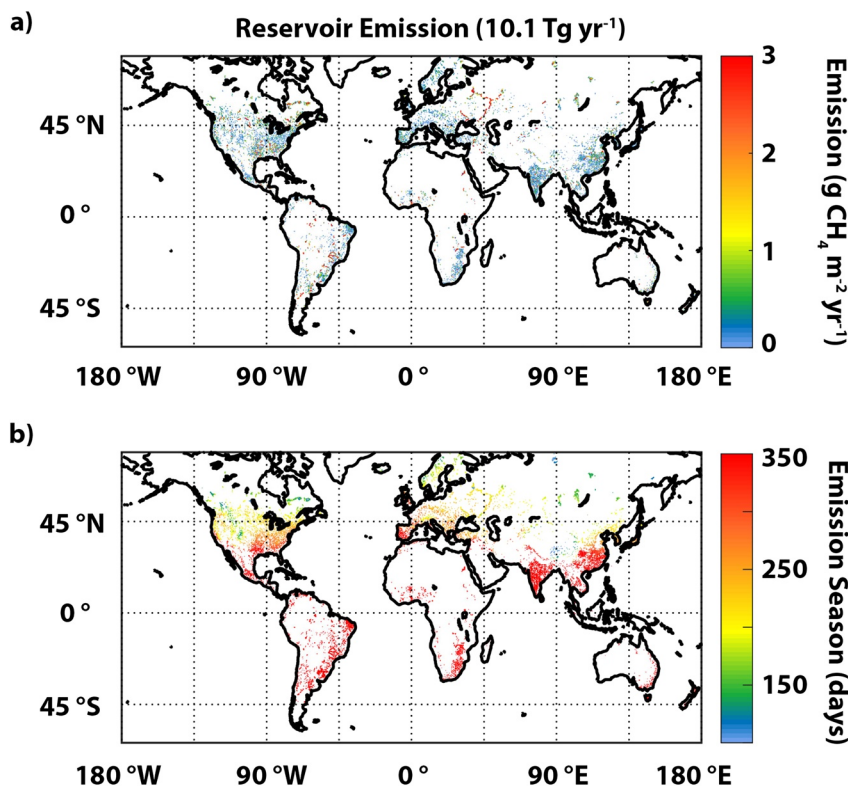


Figure 3. Global annual reservoir (a) CH₄ emission and (b) emission season length.

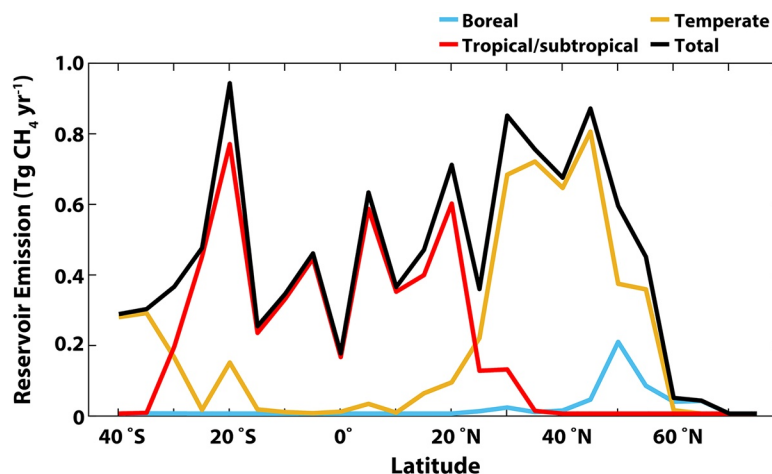


Figure 4. Zonal sums (5° latitude bins, x-axis label represents the southern limit of bins) of total reservoir CH₄ emission by eco-climatic type.

3.2.4. CH₄ Emission Seasonality

The spatial distribution of reservoir thaw/emission season length is shown in Figure 3 and mean season lengths for reservoir eco-climate types are listed in Table 1. CH₄ emission seasons for reservoirs range from <100 days in the boreal regions to 365 days in the tropics. Boreal, temperate, and tropical/subtropical reservoirs experience average emission seasons of 167, 282, and 363 days, respectively (see Table 1). In the high northern latitudes between 50° and 70°N, reservoir emissions start in late April and end in November with maximum emission rates ~ 0.01 Tg CH₄ day⁻¹ in July (see Figure 5). Between 30° and 50°N, reser-

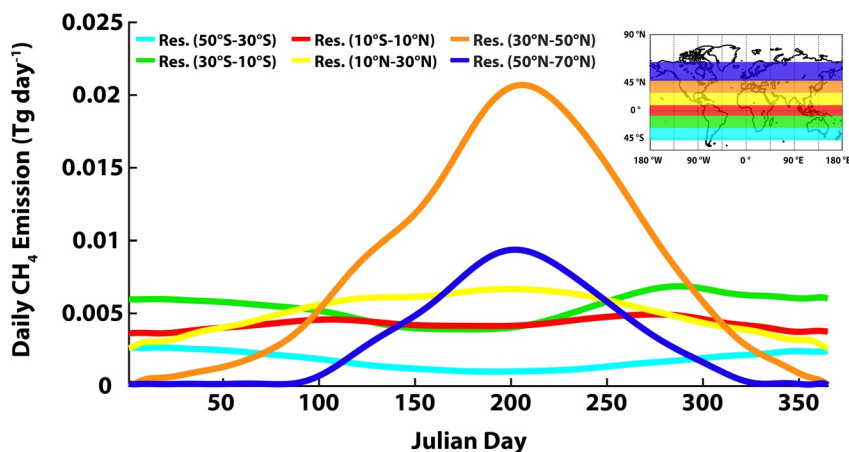


Figure 5. Daily zonal sums (20° latitude bins) of total reservoir CH_4 emission. The figure presents the polynomial curve fit of daily emissions for each latitude zone.

voirs display increasing emissions throughout the spring with maximum emissions in July and August ($\sim 0.02 \text{ Tg CH}_4 \text{ day}^{-1}$) followed by a steady decrease throughout the fall and early winter. Reservoirs in these temperate latitudes display the highest daily emissions due to the large number of systems in this region and moderate emission season length. Reservoirs located in tropical/subtropical regions of the Northern Hemisphere ($10^\circ\text{--}30^\circ\text{N}$) have lower emissions and muted seasonality compared to reservoirs farther north due to long emission seasons and lower reservoir area in these latitudes. Near the equator ($10^\circ\text{S}\text{--}10^\circ\text{N}$), CH_4 emissions from reservoirs are relatively constant year-round ($\sim 0.005 \text{ Tg CH}_4 \text{ day}^{-1}$). In the tropical/subtropical region of the Southern Hemisphere ($30^\circ\text{--}10^\circ\text{S}$), emissions display minimal seasonality, with CH_4 fluxes ranging between 0.005 and $0.075 \text{ Tg CH}_4 \text{ day}^{-1}$. Finally, low emissions occur between 50°S and 30°S with emission values between 0.001 to $0.003 \text{ Tg CH}_4 \text{ day}^{-1}$, and a maximum occurring in the Southern Hemisphere summer months.

The seasonality of emissions modeled for the ice-free season largely reflects the temperature-based corrections implemented in this study and, accordingly, emissions are highest during the warmest times of the year. Our measurement synthesis includes 32 studies reporting year-long observations, but most measurements were made during the summer season (85 observations between June and August) and the least were obtained during the winter (12 observations between December and February). Similar numbers of observations were obtained during the spring (36 observations between March and May) and fall (33 observations between September and November). Given the limited number of studies with year-round data, the role of episodic events is not explicitly captured in this emission estimate, although measured ebullitive fluxes capture some episodic fluxes. Episodic events associated with drops in atmospheric pressure (Deshmukh et al., 2014), water-level fluctuations (Harrison et al., 2017), and ice melt (Denfeld et al., 2018; Duchemin et al., 2006; Karlsson et al., 2013; Jammot et al., 2015; Jansen et al., 2019; Phelps et al., 1998) can play important roles in lake and reservoir CH_4 budgets, underscoring the need to measure these CH_4 fluxes continuously over annual and longer time periods.

3.3. Comparison With Other Reservoir CH_4 Emission Estimates

To the best of our knowledge, six global CH_4 emission estimates for reservoirs, including this study, have been published. Our estimate of $10.1 \text{ Tg CH}_4 \text{ yr}^{-1}$ is lower than other studies which report global emissions of $18\text{--}70 \text{ Tg CH}_4 \text{ yr}^{-1}$ ($12\text{--}70 \text{ Tg CH}_4 \text{ yr}^{-1}$ when considering uncertainty ranges) (see Table 2). The recent study by Harrison et al. (2021) estimated an annual global diffusive + ebullitive CH_4 emission of $9.9 \text{ Tg CH}_4 \text{ yr}^{-1}$ which is highly consistent to our study. Both studies incorporated seasonal corrections for ice-cover (satellite-derived in this study and using modeled air temperature in Harrison et al. [2021]) and temperature; however, the studies differed in their treatment of both diffusive fluxes (corrections for littoral fraction and for ice-out in Harrison et al. [2021] but not in our study) and diel variability (factored for in

Table 2
Studies of Global Reservoir CH₄ Emissions

Study	Area (10 ³ km ²)	Emission (Tg yr ⁻¹)	Comments
St. Louis et al. (2000)	1,500	70	Area from ICOLD (1988, 1998) scaled to 1,500 × 10 ³ km ² . Assumed emission season length of 200 days for temperate reservoirs, 365 days for tropical/subtropical systems. Estimate is for diffusion and ebullition.
Bastviken et al. (2011)	500	20	Area from ICOLD (2006). Emission season length, if unknown, assumed for each reservoir system based on location; no season lengths reported. Estimates for diffusion and ebullition pathways provided for some latitude regions.
Deemer et al. (2016)	306	18 (2σ range: 12–30)	Area from Lehner et al. (2011) ^a excluding regulated natural lakes. Assumed emission season length of 365 days for all reservoirs. Estimate is for diffusion and ebullition.
Rosentreter et al. (2021)	260–580	24 (mean), 15 (median)	Area simulated using Monte Carlo assuming a uniform distribution ranging between estimates from Downing et al. (2006) and Lehner et al. (2011) ^a . Ice-cover correction for waterbodies experiencing <0°C based on Fick and Hijmans (2017). Turnover correction based on Denfeld et al. (2018). Estimate is for diffusion and ebullition.
Harrison et al. (2021)	350	22	Area and distribution modeled using a subset of Lehner et al. (2011) ^a excluding four large regulated natural lakes; plus ~100 × 10 ³ km ² for small reservoirs. CH ₄ fluxes estimated using the G-Res model (Prairie et al., 2017). Simple ice-correction for ebullitive emissions when air temp. is <0°C and diffusive emissions when air temp. <4°C; no season lengths reported. Under-ice diffusive flux applied at ice-out. Seasonal flux variation modeled from temperature and reservoirs classified into eco-climatic types. Emissions from diffusion (1.6 Tg), ebullition (8.3), and degassing (12.1 Tg) pathways.
This study	297	10 (1σ range: 7–13)	Area and distribution from HydroLAKES (Messenger et al., 2016) at GRanD ^a reservoir locations (excluding regulated natural lakes) and CCI-IW at GOOD2 locations. Daily CH ₄ fluxes estimated using eco-climate reservoir type emission rates and diel corrections. Seasonal flux variation modeled from temperature. Reservoir distribution and flux sites classified into eco-climatic types; emission-season timing and duration from satellite observations. Mean season lengths = 167 days (boreal), 283 days (temperate) and 363 days (tropical/subtropical). Estimates for diffusion (1.2 Tg) and ebullition (8.9 Tg) pathways.

^aReservoir areas from Lehner et al. (2011), HydroLAKES (Messenger et al., 2016), and GRanD are the same data.

our study but not in Harrison et al. [2021]). It should be noted that both studies used air temperature as a proxy for the temperature at the air-water and sediment-water interface (where a majority of reservoir CH₄ is produced). Improving our capacity to model the stratification and sediment temperature regime of lakes and reservoirs is an important research frontier.

Estimates of total global reservoir area have varied amongst studies, contributing to differences in global reservoir emission estimates. The largest global reservoir estimate of 70 Tg CH₄ yr⁻¹ (St. Louis et al., 2000) employed a global surface area of $\sim 1,500 \times 10^3$ km² which is a factor of five larger than our study (Table 2). They cite ICOLD (1988, 1998) for an area of $\sim 500 \times 10^3$ km², but tripled that number to account for the areal underestimate they believe exists in the data set. The season lengths used in that study are somewhat similar to those in this work, meaning that the anomalously high emission estimate is directly related to the high areas. Bastviken et al. (2011) used the same $\sim 500 \times 10^3$ km² area extracted from ICOLD (2006) without adjustment and reported a total emission of 20 Tg CH₄ yr⁻¹. Compared to our results, the areas and resulting CH₄ emission estimate in Bastviken et al. (2011) are larger by $\sim 70\%$ and $\sim 100\%$, respectively suggesting that area may play a substantial role in emission differences. Deemer et al. (2016) and our study apply similar areas ($\sim 300 \times 10^3$ km²) and diffusive and ebullitive flux compilations, but estimated emissions differ by nearly a factor of two (18 and 10 Tg CH₄ yr⁻¹, respectively) due to differences between estimated and observed emission season lengths (365 days vs. a global mean of 200 days, respectively) (Table 2). Emission season lengths for high latitude lakes derived with satellite data are also noticeably shorter (by 9%–32%) than those assumed in other lake studies (Wik et al., 2016). Harrison et al. (2021) recently reported total emissions of 22 Tg CH₄ yr⁻¹ from 350×10^3 km² of global reservoir areas (comprising 1.6 Tg CH₄ yr⁻¹ via diffusion and 8.3 Tg CH₄ yr⁻¹ via ebullition). The 9.9 Tg CH₄ yr⁻¹ from diffusion + ebullition emission pathways is almost identical to our results although the spatial distributions may differ. Degassing alone accounts for $\sim 55\%$ of the global total from Harrison et al. (2021) but this study indicates that this pathway is very uncertain, flux observations are limited, and methods to characterize reservoirs and management should be improved.

Another reason that our global reservoir CH₄ emissions are lower than most previous studies is our improved accounting of diurnal emission patterns and seasonality driven by temperature-corrected eco-climatic system fluxes and freeze-thaw dynamics. St. Louis et al. (2000), Bastviken et al. (2011), and Deemer et al. (2016) derived total (diffusion + ebullition) CH₄ fluxes from 22, 35, and 161 reservoir systems, respectively. Our study incorporates measurements from the same 161 reservoir systems of Deemer et al. (2016) but we used additional measurement data from the original publications to derive true 24-h and temperature-corrected fluxes. Using different measurement compilations to derive reservoir CH₄ emissions results in variable averaged emission rates: 20 mg CH₄ m⁻² day⁻¹ and 300 mg CH₄ m⁻² day⁻¹ for temperate and tropical reservoirs in St. Louis et al. (2000); latitudinally averaged emissions ranging from 22 to 247 mg CH₄ m⁻² day⁻¹ in Bastviken et al. (2011); 160 mg CH₄ m⁻² day⁻¹ for all reservoirs in Deemer et al. (2016); and monthly average values for boreal (5–68 mg CH₄ m⁻² day⁻¹), temperate (42–259 mg CH₄ m⁻² day⁻¹), and tropical/subtropical (69–202 mg CH₄ m⁻² day⁻¹) reservoirs in this study.

In addition to different eco-climatic zone reservoir emission rates applied in past studies, the methods used to define the spatial distribution of reservoir type areas has varied. In the past these definitions have typically been done using simple latitudinal band assumptions (e.g., Bastviken et al., 2011; Deemer et al., 2016; Harrison et al., 2021); however, our study used modeled soil-temperature, which may better reflect sediment temperature, to define the spatial distribution of reservoir eco-climate type. Both our study and Harrison et al. (2021) calculated global diffusive + ebullitive CH₄ emissions ~ 10 Tg CH₄ yr⁻¹ but differ in the fractional contribution of boreal, temperate, and tropical/subtropical reservoirs. The different methods applied in this study and Harrison et al. (2021) to classify reservoir types likely resulted in these differences in reservoir eco-climatic type contribution to total emissions. This suggests that determining the best practices to define reservoir types that align with flux observations is needed in future research.

Table 2 summarizes the assumptions made for emission season lengths among the six global reservoir emission studies. Our work is unique in that satellite observations of freeze/thaw dynamics and lake-ice phenology were employed to quantify spatially varying emission season lengths, thereby addressing a major uncertainty in estimates of reservoir and lake emissions. Prior to this study, it was commonplace to assume constant emission-season lengths (Deemer et al., 2016; St. Louis et al., 2000) or simple assumptions for indi-

vidual reservoir systems (Bastviken et al., 2011) whereas Rosentreter et al. (2021) and Harrison et al. (2021) defined emission periods using air temperature for reservoirs $>0^{\circ}\text{C}$ ($>4^{\circ}\text{C}$ for diffusion in Harrison et al. (2021)) and ice-cover periods for those locations $<0^{\circ}\text{C}$ (Table 2). Specific season lengths are not reported for either of these studies.

The fact that our estimate is on the lower end of reservoir CH_4 emission estimates is both reasonable and encouraging as Saunio et al. (2020) suggests that bottom-up estimates of natural sources of CH_4 other than wetlands, that is, inland aquatic systems such as reservoirs and lakes, are substantially higher than those arrived at from top-down inverse model simulations.

3.4. Recommendations for Future Work

It should be noted that several uncertainties remain in our new data set. Additional and more systematic work focusing on data acquisition and methodological investigations is needed to better constrain reservoir CH_4 emissions.

Although we attempted to capture realistic reservoir areas, including $\sim 35,000$ small reservoirs not included in published data sources, the abundance and area of very small impoundments ($<0.1 \text{ km}^2$), that can exhibit high per m^2 emissions (e.g., Grinham et al., 2018), remain poorly represented despite a growing number of small hydropower projects (Couto & Olden, 2018). The major challenge regarding these small reservoirs is that while high-resolution remote-sensing offers the most promising approach to detecting these water bodies, it comes with the liability that numerous features that may be lakes, wetlands, or other unidentified landscape features that are not reservoirs (Matthews et al., 2020), are captured and, to date, no broadly applicable techniques have been developed to reliably distinguish among these aquatic systems. In addition, regional differences in what constitutes a regulated lake in GRanD and to what extent these systems should be considered reservoirs is an open question. Finally, this work and other studies of global reservoir emissions focus only on diffusive and ebullitive emissions, not accounting for additional emission pathways. A recent paper (Harrison et al., 2021) attributes over half of the total reservoir CH_4 flux to degassing (Table 2), suggesting the importance of better constraining this flux pathway in future modeling efforts.

The eco-climatic zones used here have been used in previous global emission efforts (Bastviken et al., 2011) and similar zones were used in Harrison et al. (2021) and the IPCC methodology for reservoir emissions (Lovelock et al., 2019). These zones implicitly integrate across multiple potential emission drivers (e.g., productivity, nutrients, temperature, and light) such that the regional influence of the physiochemical variables is already partly included in global assessments to the extent that their influence is represented in the flux measurements of the eco-climatic regions. Recent work shows a positive correlation between reservoir productivity (e.g., chlorophyll-a, nutrients) and reservoir CH_4 emissions (Deemer et al., 2016; Deemer & Holgerson, 2021; DelSontro et al., 2018). This relationship has recently been used together with global satellite-based estimates of lake and reservoir productivity to model CH_4 emissions from these aquatic systems (DelSontro et al., 2018; Rosentreter et al., 2021). However, this exercise relies on chlorophyll-a data from a single day (Sayers et al., 2015), while chlorophyll is highly variable based on dynamic relationships between nutrients and light access and top-down food web control by grazing (Wetzel, 2001). More systematic spatiotemporally resolved measurements of CH_4 emission, together with a suite of potential predictor variables, would help to better tease apart these relationships. The ability to resolve variations in spatial and temporal relationships between different pathways of CH_4 fluxes and more easily measured predictor variables (e.g., chlorophyll-a, nutrients, dissolved organic carbon) is an important topic for future work.

We note that this study incorporated 53, 81, and 64 independent time of day and temperature-corrected flux measurements for boreal, temperate, and tropical/subtropical reservoirs, respectively. Additional measurements in both tropical/subtropical and temperate reservoirs are needed to reduce uncertainties in spatial variations of CH_4 fluxes. Moreover, while boreal reservoirs are currently small contributors to the global total, amplified warming in the high latitudes suggests that strategic measurements of boreal reservoir fluxes would be useful. The augmented compilation of flux observations developed in this study contained 287 observations for diffusive and ebullition fluxes but $\sim 30\%$ of them could not be used because they lacked site information crucial to modeling diurnal and seasonal impacts on flux variability. Comprehensive site

descriptions are critical components of field studies and can greatly expand the use and value of the flux observations for modeling based on identified relationships (e.g., Deemer et al., 2016; DelSontro et al., 2018; Prairie et al., 2017) as well as for developing novel relationships with additional variables such as water depth, nutrients, and primary productivity.

Our flux compilation includes 32 year-long observations, but most reservoir-flux observations are conducted in summer months likely reflecting highest fluxes. Winter CH₄ emissions are minimally quantified, while a moderate number of observations are available for spring and fall. Consequently, to correct for the high summer flux bias, we modeled monthly mean fluxes for every measurement site based on temperature as done by Harrison et al. (2021) for individual reservoirs. More generally, flux observations vary widely in both temporal and spatial coverage. Lower spatiotemporal coverage can lead to biases in overall site emission estimates (Wik et al., 2016), but the time intensive requirements of more frequent sampling make it unrealistic in practice. However, reducing uncertainties in flux dynamics will require more spatiotemporal coverage of observational data to capture episodic fluxes and to represent the full annual cycle.

We propose that measurement data generated in the future be consistent, as much as possible, in methodology, and systematically cover multiple flux pathways and spatiotemporal variability within and among reservoirs, and include comprehensive site data. Moreover, measurement data that isolate flux pathways (e.g., diffusive, ebullitive, and alternative) and additional measurement (e.g., time of day, and date) and physiochemical (e.g., air/water temperature, chlorophyll-a, nutrients, and dissolved organic carbon) variables are helpful for modeling efforts given that their regulation, and thereby modeling requirements, differ.

4. Significance and Conclusions

Here, we present a suite of new global data sets developed during this work that combine multiple, complementary data products. These data sets are gridded at 0.25° × 0.25° spatial resolution and represent reservoir area and spatial distribution, eco-climatic reservoir type, and daily CH₄ emissions throughout the entire annual cycle. The spatial and temporal resolution of these data are uniquely aimed for use in bottom-up biogeochemical models and top-down atmospheric inverse models.

We estimate global reservoir area to be $296.6 \times 10^3 \text{ km}^2$ and total annual emission of $10.1 \text{ Tg CH}_4 \text{ yr}^{-1}$ (1 σ uncertainty range of 7.2–12.9 Tg CH₄ yr⁻¹) for diffusion (1.2 Tg CH₄ yr⁻¹) and ebullition (8.9 Tg CH₄ yr⁻¹) pathways. This total emission is lower than most past estimates, and similar to the results from Harrison et al. (2021) for the same pathways (Table 2). Our global total emission is on the low end of estimates due primarily to shorter emission seasons derived from satellite observations, lower areas representing only true reservoirs, diel corrections to daily CH₄ fluxes to account for lower nighttime emissions, seasonal fluxes calculated from daily emission rates to reflect impacts of temperature fluctuations, and application of region-specific fluxes to eco-climatic reservoir types. These results indicate that simple assumptions about temporal and spatial variability employed in previous studies result in the larger estimates of reservoir emissions associated with diffusive and ebullitive fluxes.

This research addresses several critical gaps and uncertainties existing in estimates of reservoir CH₄ emissions to date. The results are tightly anchored in field observations, in situ measurements, and remote-sensing observations independent of diagnostic or prognostic models (e.g., ecosystem and/or biogeochemical models) and integrate impacts of diel, temperature-, and ice-cover variability on emissions.

This work represents important data and methodological contributions to better constrain global CH₄ modeling and budget assessments for the present, and the recent past, while also providing a framework for predicting future reservoir emissions that may result from changes in climate. Reservoirs are projected to become more numerous in the future due to the increased need for sustainable energy from hydropower and water storage for irrigation (Zarfl et al., 2015). For example, hundreds of new reservoirs are planned in the Amazon basin (Almeida et al., 2019) which already exhibits large reservoir emissions due to year-long emission seasons and warm air and water temperatures. By quantifying spatiotemporal emission dynamics and supporting scenario analyses, this work can be employed in strategic planning of reservoir placement and design to minimize future reservoir emissions.

The spatially and temporally explicit analysis reported here represents important progress toward expanding the understanding and reducing uncertainties in the global CH₄ budget and enabling the inclusion of reservoir fluxes in an array of biogeochemical, top-down inverse atmospheric, and Earth System models.

Conflict of Interest

The authors perceive no financial, or other affiliations, which are conflicts of interest.

Data Availability Statement

The gridded data sets produced in this study can be downloaded from NASA's Oak Ridge National Laboratory Distributed Active Archive Center (<https://doi.org/10.3334/ORNLDAAAC/1918>). The reservoir CH₄ flux compilation derived in this study is included with this manuscript as Data Set S1. Data used for producing the remote-sensing freeze/thaw information applied in this study were downloaded from NASA's National Snow and Ice Data Center Distributed Active Archive Center (lake-ice phenology: <https://doi.org/10.5067/HT4NQ07ZJF7M> and landscape freeze/thaw: <https://doi.org/10.5067/MEASURES/CRYOSPHERE/nsidc-0477.004>; last access: 12/01/2020). The authors acknowledge the data used to produce reservoir area data from GRanD (<http://sedac.ciesin.columbia.edu/pfs/grand.html>; last access: 9/13/2020), GOOD2 (<http://geodata.policysupport.org/dams>; last access: 9/02/2020), and CCI-IW (<https://www.esa-landcover-cci.org/?q=node/180>; last access: 07/20/2021). The authors also acknowledge the usage of the publicly available MERRA-2 meteorology and soil temperature data downloaded from NASA's EarthData repository (<https://earthdata.nasa.gov/>; last access: 11/10/2020).

Acknowledgments

M. Johnson, E. Matthews, and V. Genovese were funded for this work by NASA's Interdisciplinary Research in Earth Science (IDS) Program and the NASA Terrestrial Ecology and Tropospheric Composition Programs. D. Bastviken was funded by the European Research Council (ERC; grant agreement No 725546). J. Du was a collaborator on the IDS project which funded the majority of this work. B. Deemer's contribution to this study was through in-kind efforts. Resources supporting this work were provided by the NASA High-End Computing (HEC) Program through the NASA Advanced Supercomputing (NAS) Division at NASA Ames Research Center. The authors acknowledge the helpful comments by two anonymous reviewers and Kyle Delwiche. Any use of trade, product, or firm names is for descriptive purposes only and does not imply endorsement by the U.S. Government. Finally, the views, opinions, and findings contained in this report are those of the authors and should not be construed as an official NASA position, policy, or decision.

References

- Aben, R. C. H., Barros, N., van Donk, E., Frenken, T., Hilt, S., Kazanjian, G., et al. (2017). Cross continental increase in methane ebullition under climate change. *Nature Communications*, 8(1), 1682. <https://doi.org/10.1038/s41467-017-01535-y>
- Almeida, R. M., Shi, Q., Gomes-Selman, J. M., Wu, X., Xue, Y., Angarita, H., et al. (2019). Reducing greenhouse gas emissions of Amazon hydropower with strategic dam planning. *Nature Communications*, 10(1), 1–9. <https://doi.org/10.1038/s41467-019-12179-5>
- Barros, N., Cole, J., Tranvik, L., Prairie, Y. T., Bastviken, D., Huszar, V. L. M., et al. (2011). Carbon emission from hydroelectric reservoirs linked to reservoir age and latitude. *Nature Geoscience*, 4, 593–596. <https://doi.org/10.1038/ngeo1211>
- Bastviken, D., Cole, J., Pace, M., & Tranvik, L. (2004). Methane emissions from lakes: Dependence on lake characteristics, two regional assessments, and a global estimate. *Global Biogeochemical Cycles*, 18, GB4009. <https://doi.org/10.1029/2004GB002238>
- Bastviken, D., Tranvik, L. J., Downing, J. A., Crill, P. M., & Enrich-Prast, A. (2011). Freshwater methane emissions offset the continental carbon sink. *Science*, 331, 50. <https://doi.org/10.1126/science.1196808>
- Bloom, A. A., Bowman, K. W., Lee, M., Turner, A. J., Schroeder, R., Worden, J. R., et al. (2017). A global wetland methane emissions and uncertainty dataset for atmospheric chemical transport models (WetCHARTs version 1.0). *Geoscientific Model Development*, 10, 2141–2156. <https://doi.org/10.5194/gmd-10-2141-2017>
- Ciais, P., Sabine, C., Bala, G., Bopp, L., Brovkin, V., Canadell, J., & Jones, C. (2013). Carbon and other biogeochemical cycles. Climate change 2013: The physical science basis. In *Contribution of working group I to the fifth assessment report of the intergovernmental panel on climate change* (pp. 465–570). Cambridge United Kingdom and New York NY: Cambridge University Press.
- Couto, T. B., & Olden, J. D. (2018). Global proliferation of small hydropower plants—Science and policy. *Frontiers in Ecology and the Environment*, 16, 91–100. <https://doi.org/10.1002/fee.1746>
- Deemer, B. R., Harrison, J. A., Li, S., Beaulieu, J. J., DelSontro, T., Barros, N., et al. (2016). Greenhouse gas emissions from reservoir water surfaces: A new global synthesis. *BioScience*, 66, 949–964. <https://doi.org/10.1093/biosci/biw117>
- Deemer, B. R., & Holgerson, M. A. (2021). Drivers of methane flux differ between lakes and reservoirs, complicating global upscaling efforts. *Journal of Geophysical Research: Biogeosciences*, 126, e2019JG005600. <https://doi.org/10.1029/2019JG005600>
- DelSontro, T., Beaulieu, J. J., & Downing, J. A. (2018). Greenhouse gas emissions from lakes and impoundments: Upscaling in the face of global change. *Limnology and Oceanography Letters*, 3, 64–75. <https://doi.org/10.1002/lol2.10073>
- Demarty, M., Bastien, J., & Tremblay, A. (2011). Annual follow-up of gross diffusive carbon dioxide and methane emissions from a boreal reservoir and two nearby lakes in Québec, Canada. *Biogeosciences*, 8, 41–53. <https://doi.org/10.5194/bg-8-41-2011>
- Denfeld, B. A., Baulch, H. M., del Giorgio, P. A., Hampton, S. E., & Karlsson, J. (2018). A synthesis of carbon dioxide and methane dynamics during the ice-covered period of northern lakes. *Limnology and Oceanography Letters*, 3, 117–131. <https://doi.org/10.1002/lol2.10079>
- Deshmukh, C., Serça, D., Delon, C., Tardif, R., Demarty, M., Jarnot, C., et al. (2014). Physical controls on CH₄ emissions from a newly flooded subtropical freshwater hydroelectric reservoir: Nam Theun 2. *Biogeosciences*, 11, 4251–4269. <https://doi.org/10.5194/bg-11-4251-2014>
- Downing, J. A., Prairie, Y. T., Cole, J. J., Duarte, C. M., Tranvik, L. J., Striegl, R. G., et al. (2006). The global abundance and size distribution of lakes, ponds, and impoundments. *Limnology and Oceanography*, 51(5), 2388–2397. <https://doi.org/10.1016/B978-012370626-3.00025-9>
- Du, J., & Kimball, J. S. (2018). Daily lake ice phenology time series derived from AMSR-E and AMSR2, Version 1. Boulder, CO. NASA National Snow and Ice Data Center Distributed Active Archive Center. <https://doi.org/10.5067/HT4NQ07ZJF7M>
- Du, J., Kimball, J. S., Duguay, C., Kim, Y., & Watts, J. D. (2017). Satellite microwave assessment of Northern Hemisphere lake ice phenology from 2002 to 2015. *Cryosphere*, 11, 47–63. <https://doi.org/10.5194/tc-11-47-2017>

- Duchemin, E., Lucotte, M., Canuel, R., & Soumis, N. (2006). First assessment of CH₄ and CO₂ emissions from shallow and deep zones of boreal reservoirs upon ice break-up. *Lakes and Reservoirs: Research and Management*, *11*, 9–19. <https://doi.org/10.1111/j.1440-1770.2006.00285.x>
- Fick, S. E., & Hijmans, R. J. (2017). WorldClim 2: New 1-km spatial resolution climate surfaces for global land areas. *International Journal of Climatology*, *37*, 4302–4315. <https://doi.org/10.1002/joc.5086>
- Gelaro, R., McCarty, W., Suarez, M. J., Todling, R., Molod, A., Takacs, L., et al. (2017). The modern-era retrospective analysis for research and applications, version 2 (MERRA-2). *Journal of Climate*, *30*(14), 5419–5454. <https://doi.org/10.1175/JCLI-D-16-0758.1>
- Grinham, A., Albert, S., Deering, N., Dunbabin, M., Bastviken, D., Sherman, B., et al. (2018). The importance of small artificial water bodies as sources of methane emissions in Queensland, Australia. *Hydrology and Earth System Sciences*, *22*, 5281–5298. <https://doi.org/10.5194/hess-22-5281-2018>
- Harrison, J. A., Deemer, B. R., Birchfield, M. K., & O'Malley, M. T. (2017). Reservoir water-level drawdowns accelerate and amplify methane emission. *Environmental Science and Technology*, *51*, 1267–1277. <https://doi.org/10.1021/acs.est.6b03185>
- Harrison, J. A., Prairie, Y. T., Mercier-Blais, S., & Soued, C. (2021). Year-2020 global distribution and pathways of reservoir methane and carbon dioxide emissions according to the greenhouse gas from reservoirs (G-res) model. *Global Biogeochemical Cycles*, *35*, e2020GB006888. <https://doi.org/10.1029/2020GB006888>
- International Commission on Large Dams (ICOLD) (1988). *World register of dams*. Paris: ICOLD. <https://www.icold-cigb.org/>
- International Commission on Large Dams (ICOLD) (2006). *World register of dams*. Paris: ICOLD. <https://www.icold-cigb.org/>
- Jammet, M., Crill, P., Dengel, S., & Friberg, T. (2015). Large methane emissions from a subarctic lake during spring thaw: Mechanisms and landscape significance. *Journal of Geophysical Research: Biogeosciences*, *120*(11), 2289–2305. <https://doi.org/10.1002/2015JG003137>
- Jansen, J., Thornton, B. F., Jammet, M. M., Wik, M., Cortes, A., Friberg, T., et al. (2019). Climate-sensitive controls on large spring emissions of CH₄ and CO₂ from northern lakes. *Journal of Geophysical Research: Biogeosciences*, *124*, 2379–2399. <https://doi.org/10.1029/2019JG005094>
- Jansen, J., Thornton, B. F., Wik, M., MacIntyre, S., & Crill, P. M. (2020). Temperature proxies as a solution to biased sampling of lake methane emissions. *Geophysical Research Letters*, *47*, e2020GL088647. <https://doi.org/10.1029/2020GL088647>
- Karlsson, J., Giesler, R., Persson, J., & Lundin, E. (2013). High emission of carbon dioxide and methane during ice thaw in high latitude lakes. *Geophysical Research Letters*, *40*, 1123–1127. <https://doi.org/10.1002/grl.50152>
- Kim, Y., Kimball, J. S., Glassy, J. M., & Du, J. (2017a). An extended global Earth system data record on daily landscape freeze–thaw status determined from satellite passive microwave remote sensing. *Earth System Science Data*, *9*, 133–147. <https://doi.org/10.5194/essd-9-133-2017>
- Kim, Y., Kimball, J. S., Glassy, J. M., & McDonald, K. C. (2017b). *MEASURES global record of daily landscape freeze/thaw status, Version 4*. Boulder, CO: NASA National Snow and Ice Data Center Distributed Active Archive Center. <https://doi.org/10.5067/MEASURES/CRYOSPHERE/nsidc-0477.004>
- Kirschke, S., Bousquet, P., Ciais, P., Saunio, M., Canadell, J. G., Dlugokencky, E. J., et al. (2013). Three decades of global methane sources and sinks. *Nature Geoscience*, *6*(10), 813–823. <https://doi.org/10.1038/ngeo1955>
- Lamarque, C., Santoro, M., Bontemps, S., d'Andrimont, R., Radoux, J., Giustarini, L., et al. (2017). Compilation and validation of SAR and optical data products for a complete and global map of inland/ocean water tailored to the climate modeling community. *Remote Sensing*, *9*, 36. <https://doi.org/10.3390/rs9010036>
- Lehner, B., & Döll, P. (2004). Development and validation of a global database of lakes, reservoirs and wetlands. *Journal of Hydrology*, *296*, 1–22. <https://doi.org/10.1016/j.jhydrol.2004.03.028>
- Lehner, B., Liermann, C. R., Revenga, C., Vörösmarty, C., Fekete, B., Crouzet, P., et al. (2011). High-resolution mapping of the world's reservoirs and dams for sustainable river-flow management. *Frontiers in Ecology and the Environment*, *9*(9), 494–502. <https://doi.org/10.1890/100125>
- Lovelock, C. E., Barros, N., Prairie, Y., Alm, J., Bastviken, D., Beaulieu, J. J., et al. (2019). Chapter 7: Wetlands. In *2019 refinement to the 2006 IPCC guidelines for National Greenhouse Gas Inventories* (pp. 7.1–7.52). Switzerland: Intergovernmental Panel on Climate Change. <https://repository.ubn.ru.nl/handle/2066/205862>
- Marotta, H., Pinho, L., Gudas, C., Bastviken, D., Tranvik, L. J., & Enrich-Prast, A. (2014). Greenhouse gas production in low-latitude lake sediments responds strongly to warming. *Nature Climate Change*, *4*, 467–470. <https://doi.org/10.1038/NCLIMATE2222>
- Matthews, E., Johnson, M. S., Genovesi, V., Du, J., & Bastviken, D. (2020). Methane emission from high latitude lakes: Methane-centric lake classification and satellite-driven annual cycle of emissions. *Scientific Reports*, *10*, 12465. <https://doi.org/10.1038/s41598-020-68246-1>
- Melton, J. R., Wania, R., Hodson, E. L., Poulter, B., Ringeval, B., Spahni, R., et al. (2013). Present state of global wetland extent and wetland methane modelling: Conclusions from a model inter-comparison project (WETCHIMP). *Biogeosciences*, *10*, 753–788. <https://doi.org/10.5194/bg-10-753-2013>
- Messenger, M. L., Lehner, B., Grill, G., Nedeva, I., & Schmitt, O. (2016). Estimating the volume and age of water stored in global lakes using a geo-statistical approach. *Nature Communications*, *7*, 13603. <https://doi.org/10.1038/ncomms13603>
- Mulligan, M., Saenz-Cruz, L., van Soesbergen, A., Smith, V. T., & Zurita, L. (2009). *Global dams database and geowiki*. (Version 1). <http://geodata.policysupport.org/dams>
- Natchimuthu, S., Sundgren, I., Gålfalk, M., Klemetsson, L., Crill, P., Danielsson, Å., & Bastviken, D. (2016). Spatio-temporal variability of lake CH₄ fluxes and its influence on annual whole lake emission estimates. *Limnology and Oceanography*, *61*(S1), S13–S26. <https://doi.org/10.1002/lno.10222>
- Petrescu, A. M. R., van Beek, L. P. H., van Huissteden, J., Prigent, C., Sachs, T., Corradi, C. A. R., et al. (2010). Modeling regional to global CH₄ emissions of boreal and arctic wetlands. *Global Biogeochemical Cycles*, *24*, GB4009. <https://doi.org/10.1029/2009GB003610>
- Phelps, A. R., Peterson, K. M., & Jeffries, O. (1998). Methane efflux from high-latitude lakes during spring ice melt. *Journal of Geophysical Research*, *103*, 29029–29036. <https://doi.org/10.1029/98JD00044>
- Podgrajsek, E., Sahlée, E., & Rutgersson, A. (2014). Diurnal cycle of lake methane flux. *Journal of Geophysical Research: Biogeosciences*, *119*, 236–248. <https://doi.org/10.1002/2013JG002327>
- Prairie, Y. T., Alm, J., Harby, A., Mercier-Blais, S., & Nahas, R. (2017). *The GHG Reservoir Tool (Gres) Technical documentation v2.1 UNE-SCO/IHA research project on the GHG status of freshwater reservoirs* (p. 76). Joint publication of the UNESCO Chair in Global Environmental Change and the International Hydropower Association.
- Rosentreter, J. A., Borges, A. V., Deemer, B. R., Holgersson, M. A., Liu, S., Song, C., et al. (2021). Half of global methane emissions come from highly variable aquatic ecosystem sources. *Nature Geoscience*, *14*, 225–230. <https://doi.org/10.1038/s41561-021-00715-2>
- Saunio, M., Bousquet, P., Poulter, B., Peregon, A., Ciais, P., Canadell, J. G., et al. (2016). The global methane budget 2000–2012. *Earth System Science Data*, *8*, 697–751. <https://doi.org/10.5194/essd-8-697-2016>

- Saunio, M., Stavert, A. R., Poulter, B., Bousquet, P., Canadell, J. G., Jackson, R. B., et al. (2020). The Global Methane Budget 2000–2017. *Earth System Science Data*, 12, 1561–1623. <https://doi.org/10.5194/essd-12-1561-2020>
- Sayers, M. J., Grimm, A. G., Shuchman, R. A., Deines, A. M., Bunnell, D. B., Raymer, Z. B., et al. (2015). A new method to generate a high-resolution global distribution map of lake chlorophyll. *International Journal of Remote Sensing*, 36(7), 1942–1964. <https://doi.org/10.1080/01431161.2015.1029099>
- Schubert, C. J., Diem, T., & Eugster, W. (2012). Methane emissions from a small wind shielded lake determined by eddy covariance, flux chambers, anchored funnels, and boundary model calculations: A comparison. *Environmental Science and Technology*, 46(8), 4515–4522. <https://doi.org/10.1021/es203465x>
- Sieczko, A. K., Duc, N. T., Schenk, J., Pajala, G., Rudberg, D., Sawakuchi, H. O., & Bastviken, D. (2020). Diel variability of methane emissions from lakes. *Proceedings of the National Academy of Sciences*, 117, 21488–21494. <https://doi.org/10.1073/pnas.2006024117>
- St. Louis, V. L., Kelly, C. A., Duchemin, É., Rudd, J. W., & Rosenberg, D. M. (2000). Reservoir surfaces as sources of greenhouse gases to the atmosphere: A global estimate. *BioScience*, 50, 766–775. [https://doi.org/10.1641/0006-3568\(2000\)050\[0766:rsasog\]2.0.co;2](https://doi.org/10.1641/0006-3568(2000)050[0766:rsasog]2.0.co;2)
- Thornton, B. F., Wik, M., & Crill, P. M. (2016). Double-counting challenges the accuracy of high-latitude methane inventories. *Geophysical Research Letters*, 43. <https://doi.org/10.1002/2016GL071772>
- Wetzel, R. G. (2001). *Limnology—Lake and river ecosystems*. Academic Press.
- Wik, M., Varner, R. K., Walter Anthony, K., MacIntyre, S., & Bastviken, D. (2016). Climate-sensitive northern lakes and ponds are critical components of methane release. *Nature Geoscience*, 9, 99–105. <https://doi.org/10.1038/ngeo2578>
- Yvon-Durocher, G., Allen, A. P., Bastviken, D., Conrad, R., Gudas, C., St-Pierre, A., et al. (2014). Methane fluxes show consistent temperature dependence across microbial to ecosystem scales. *Nature*, 507, 488–491. <https://doi.org/10.1038/nature13164>
- Zarfl, C., Lumsdon, A. E., Berlekamp, J., Tydecks, L., & Tockner, K. (2015). A global boom in hydropower dam construction. *Aquatic Sciences*, 77(1), 161–170. <https://doi.org/10.1007/s00027-014-0377-0>
- Zhang, K., Kimball, J. S., Kim, Y., & McDonald, K. C. (2011). Changing freeze-thaw seasons in northern high latitudes and associated influences on evapotranspiration. *Hydrological Processes*, 25(26), 4142–4151. <https://doi.org/10.1002/hyp.8350>

References From the Supporting Information

- Abril, G., Guérin, F., Richard, S., Delmas, R., Galy-Lacaux, C., Gosse, P., et al. (2005). Carbon dioxide and methane emissions and the carbon budget of a 10-year old tropical reservoir (Petit Saut, French Guiana). *Global Biogeochemical Cycles*, 19, GB4007. <https://doi.org/10.1029/2005GB002457>
- Almeida, R. M., Nóbrega, G. N., Junger, P. C., Figueiredo, A. V., Andrade, A. S., de Moura, C. G. B., et al. (2016). High primary production contrasts with intense carbon emission in a eutrophic tropical reservoir. *Frontiers in Microbiology*, 7, 717. <https://doi.org/10.3389/fmicb.2016.00717>
- Andrade, G. de S. D. (2014). *Greenhouse gas emission (GHG) and atmospheric impacts accrue from hydroelectricity production: Case study of Volta Grande hydropower plant*. (PhD Thesis). Universidade Federal de Minas Gerais.
- Bansal, S., Chakraborty, M., Katyal, D., & Garg, J. K. (2015). Methane flux from a subtropical reservoir located in the floodplains of river Yamuna, India. *Applied Ecology and Environmental Research*, 13, 597–613. https://doi.org/10.15666/aeer/1302_597613
- Barros, N., Cole, J. J., Tranvik, L. J., Prairie, Y. T., Bastviken, D., Huszar, V. L. M., et al. (2011). Carbon emission from hydroelectric reservoirs linked to reservoir age and latitude. *Nature Geoscience*, 4(9), 593–596. <https://doi.org/10.1038/ngeo1211>
- Bastviken, D., Tranvik, L. J., Downing, J. A., Crill, P. M., & Enrich-Prast, A. (2011). Freshwater methane emissions offset the continental carbon sink. *Science*, 331(6013), 50. <https://doi.org/10.1126/science.1196808>
- Beaulieu, J. J., Smolenski, R. L., Nietch, C. T., Townsend-Small, A., & Elovitz, M. S. (2014). High methane emissions from a midlatitude reservoir draining an agricultural watershed. *Environmental Science and Technology*, 48(19), 11100–11108. <https://doi.org/10.1021/es501871g>
- Bergier, I., Novo, E. M. L. M., Ramos, F. M., Mazzi, E. A., & Rasera, M. F. F. L. (2011). Carbon dioxide and methane fluxes in the littoral zone of a tropical savanna reservoir (Corumbá, Brazil). *Oecologia Australis*, 15(3), 666–681. <https://doi.org/10.4257/oeco.2011.1503.17>
- Bevelhimer, M. S., Stewart, A. J., Fortner, A. M., Phillips, J. R., & Mosher, J. J. (2016). CO₂ is dominant greenhouse gas emitted from six hydropower reservoirs in southeastern United States during peak summer emissions. *Watermark*, 8, 14. <https://doi.org/10.3390/w8010015>
- Chanudet-Descloux, V. S., Harby, A., Sundt, H., Hansen, B. H., Brakstad, O., Serça, D., & Guerin, F. (2011). Gross CO₂ and CH₄ emissions from the Nam Ngum and Nam Leuk sub-tropical reservoirs in Lao PDR. *Science of the Total Environment*, 409, 5382–5391. <https://doi.org/10.1016/j.scitotenv.2011.09.018>
- Chen, H., Yuan, X., Chen, Z., Wu, Y., Liu, X., Zhu, D., et al. (2011). Methane emissions from the surface of the Three Gorges Reservoir. *Journal of Geophysical Research*, 116, D21306. <https://doi.org/10.1029/2011JD016244>
- Delontro, T., Kunz, M. J., Kempter, T., Wüest, A., Wehrli, B., & Senn, D. B. (2011). Spatial heterogeneity of methane ebullition in a large tropical reservoir. *Environmental Science and Technology*, 45(23), 9866–9873. <https://doi.org/10.1021/es2005545>
- DelSontro, T., McGinnis, D. F., Sobek, S., Ostrovsky, I., & Wehrli, B. (2010). Extreme methane emissions from a Swiss hydropower reservoir: Contribution from bubbling sediments. *Environmental Science and Technology*, 44(7), 2419–2425. <https://doi.org/10.1021/es9031369>
- Demarty, M., Bastien, J., Tremblay, A., Hesslein, R. H., & Gill, R. (2009). Greenhouse gas emissions from boreal reservoirs in Manitoba and Québec, Canada, measured with automated systems. *Environmental Science and Technology*, 43, 8908–8915. <https://doi.org/10.1021/es8035658>
- De Mello, N., Brighenti, L. S., Barbosa, F. A. R., Staehr, P. A., & Neto, J. F. B. (2018). Spatial variability of methane (CH₄) ebullition in a tropical hypereutrophic reservoir: Silted areas as a bubble hot spot. *Lake and Reservoir Management*, 34(2), 105–114. <https://doi.org/10.1080/10402381.2017.1390018>
- Deshmukh, C., Serça, D., Delon, C., Tardif, R., Demarty, M., Jarnot, C., et al. (2014). Physical controls on CH₄ emissions from a newly flooded subtropical freshwater hydroelectric reservoir: Nam Theun 2. *Biogeosciences*, 11, 4251–4269. <https://doi.org/10.5194/bg-11-4251-2014>
- Diem, T., Koch, S., Schwarzenbach, S., Wehrli, B., & Schubert, C. J. (2012). Greenhouse gas emissions (CO₂, CH₄, and N₂O) from several perialpine and alpine hydropower reservoirs by diffusion and loss in turbines. *Aquatic Sciences*, 74(3), 619–635. <https://doi.org/10.1007/s00027-012-0256-5>
- dos Santos, M. A., Rosa, L. P., Sikar, B., Sikar, E., & dos Santos, E. O. (2006). Gross greenhouse gas fluxes from hydro-power reservoir compared to thermo-power plants. *Energy Policy*, 34, 481–488.
- Duchemin, É., Lucotte, M., Canuel, R., & Chamberland, A. (1995). Production of the greenhouse gases CH₄ and CO₂ by hydroelectric reservoirs of the boreal region. *Global Biogeochemical Cycles*, 9, 529–540. <https://doi.org/10.1029/95GB02202>

- Fedorov, M. P., Elistratov, V. V., Maslikov, V. I., Sidorenko, G. I., Chusov, A. N., Atrashenok, V. P., et al. (2015). Reservoir greenhouse gas emissions at Russian HPP. *Power Technology and Engineering*, 49, 33–39.
- Gonzalez-Valencia, R., Magana-Rodriguez, F., Gerardo-Nieto, O., Sepulveda-Jauregui, A., Martinez-Cruz, K., Walter Anthony, K., et al. (2014). In situ measurement of dissolved methane and carbon dioxide in freshwater ecosystems by off-axis integrated cavity output spectroscopy. *Environmental Science and Technology*, 48(19), 11421–11428. <https://doi.org/10.1021/es500987j>
- Grinham, A., Dunbabin, M., Gale, D., & Udy, J. (2011). Quantification of ebullitive and diffusive methane release to atmosphere from a water storage. *Atmospheric Environment*, 45(39), 7166–7173. <https://doi.org/10.1016/j.atmosenv.2011.09.011>
- Gruca-Rokosz, R. (2020). Quantitative fluxes of the greenhouse gases CH₄ and CO₂ from the surfaces of selected Polish reservoirs. *Atmosphere*, 11, 286. <https://doi.org/10.3390/atmos11030286>
- Gruca-Rokosz, R., Tomaszek, J., Koszelnik, P., & Czerwieniec, E. (2010). Methane and carbon dioxide emission from some reservoirs in SE Poland. *Limnological Review*, 10, 15–21.
- Guérin, F., Abril, G., Richard, S., Burban, B., Reynouard, C., Seyler, P., & Delmas, R. (2006). Methane and carbon dioxide emissions from tropical reservoirs: Significance of downstream rivers. *Geophysical Research Letters*, 33, L21407. <https://doi.org/10.1029/2006GL027929>
- Harrison, J. A., Deemer, B. R., Birchfield, M. K., & O'Malley, M. T. (2017). Reservoir water-level drawdowns accelerate and amplify methane emission. *Environmental Science and Technology*, 51(3), 1267–1277. <https://doi.org/10.1021/acs.est.6b03185>
- Huttunen, J. T., Alm, J., Liikainen, A., Juutinen, S., Larmola, T., Hammar, T., et al. (2003). Fluxes of methane, carbon dioxide and nitrous oxide in boreal lakes and potential anthropogenic effects on the aquatic greenhouse gas emissions. *Chemosphere*, 52(3), 609–621. [https://doi.org/10.1016/s0045-6535\(03\)00243-1](https://doi.org/10.1016/s0045-6535(03)00243-1)
- Itoh, M., Kobayashi, Y., Chen, T. Y., Tokida, T., Fukui, M., Kojima, H., et al. (2015). Effect of interannual variation in winter vertical mixing on CH₄ dynamics in a subtropical reservoir. *Journal of Geophysical Research: Biogeosciences*, 120, 1246–1261. <https://doi.org/10.1002/2015JG002972>
- Jacinto, P. A., Filippelli, G. M., Tedesco, L. P., & Raftis, R. (2012). Carbon storage and greenhouse gases emission from a fluvial reservoir in an agricultural landscape. *Catena*, 94, 53–63. <https://doi.org/10.1016/j.catena.2011.03.012>
- Joyce, J., & Jewell, P. W. (2003). Physical controls on methane ebullition from reservoirs and lake. *Environmental and Engineering Geoscience*, 9(2), 167–178. <https://doi.org/10.2113/9.2.167>
- Keller, M., & Stallard, R. F. (1994). Methane emission by bubbling from Gatun Lake, Panama. *Journal of Geophysical Research*, 99(D4), 8307–8319. <https://doi.org/10.1029/92JD02170>
- Kelly, C. A., Rudd, J. W., St Louis, V. L., & Moore, T. (1994). Turning attention to reservoir surfaces, a neglected area in greenhouse studies. *Eos Transactions American Geophysical Union*, 75, 332–333.
- Kelly, C. A., Rudd, J. W. M., Bodaly, R. A., Roulet, N. P., St Louis, V. L., Heyes, A., et al. (1997). Increases in fluxes of greenhouse gases and methyl mercury following flooding of an experimental reservoir. *Environmental Science and Technology*, 31, 1334–1344.
- Kemenes, A., Forsberg, B. R., & Melack, J. M. (2007). Methane release below a tropical hydroelectric dam. *Geophysical Research Letters*, 34, L12809. <https://doi.org/10.1029/2007GL029479>
- Kumar, A., & Sharma, M. P. (2016). Assessment of risk of GHG emissions from Tehri hydropower reservoir, India. *Human and Ecological Risk Assessment*, 22, 71–85.
- Li, S., Zhang, Q., Bush, R. T., & Sullivan, L. A. (2015). Methane and CO₂ emissions from China's hydroelectric reservoirs: A new quantitative synthesis. *Environmental Science and Pollution Research*, 22, 5325–5339.
- Lima, I. B. T. (2005). Biogeochemical distinction of methane releases from two Amazon hydro-reservoirs. *Chemosphere*, 59, 1697–1702.
- Lima, I. B. T., de Moraes Novo, E. M. L., Ballester, M. V. R., & Ometto, J. P. (1998). Methane production, transport and emission in Amazon hydroelectric plants. In *Geoscience and remote sensing symposium proceedings, IGARSS'98. 1998 IEEE international*. (Vol. 5, pp. 2529–2531). IEEE.
- Lima, I. B. T., Victoria, R. L., Novo, E. M. L. M., Freigl, B. J., Ballester, M. V. R., & Ometto, J. P. (2002). Methane, carbon dioxide and nitrous oxide emissions from two Amazonian reservoirs during high water table. *International Society of Limnology*, 28, 438–442.
- Lu, F., Yang, L., Wang, X., Duan, X., Mu, Y., Song, W., et al. (2011). Preliminary report on methane (CH₄) emissions from the Three Gorges Reservoir (TGR) in the summer drainage period. *Journal of Environmental Sciences*, 23(12), 2029–2033. [https://doi.org/10.1016/S1001-0742\(10\)60668-7](https://doi.org/10.1016/S1001-0742(10)60668-7)
- Maeck, A., DelSontro, T., McGinnis, D. F., Fischer, H., Flury, S., Schmidt, M., et al. (2013). Sediment trapping by dams creates methane emission hot spots. *Environmental Science and Technology*, 47(15), 8130–8137. <https://doi.org/10.1021/es4003907>
- Maeck, A., Hofmann, H., & Lorke, A. (2014). Pumping methane out of aquatic sediments—Ebullition forcing mechanisms in an impounded river. *Biogeosciences*, 11(11), 2925–2938. <https://doi.org/10.5194/bg-11-2925-2014>
- Marcelino, A. A., Santos, M. A., Xavier, V. L., Bezerra, C. S., Silva, C. R. O., Amorim, M. A., & Rogerio, J. P. (2015). Diffusive emission of methane and carbon dioxide from two hydropower reservoirs in Brazil. *Brazilian Journal of Biology*, 75(2), 331–338. <https://doi.org/10.1590/1519-6984.12313>
- Musenze, R. S., Grinham, A., Werner, U., Gale, D., Sturm, K., Udy, J., & Yuan, Z. (2014). Assessing the spatial and temporal variability of diffusive methane and nitrous oxide emissions from subtropical freshwater reservoirs. *Environmental Science & Technology*, 48(24), 14499–14507. <https://doi.org/10.1021/es505324h>
- Ometto, J. P., Cimblaris, A. C. P., dos Santos, M. A., Rosa, L. P., Abe, D., Tundisi, J. G., et al. (2013). Carbon emission as a function of energy generation in hydroelectric reservoirs in Brazilian dry tropical biome. *Energy Policy*, 58(C), 109–116. <https://doi.org/10.1016/j.enpol.2013.02.041>
- Rosa, L. P., dos Santos, M. A., Matvienko, B., dos Santos, E. O., & Sikar, E. (2004). Greenhouse gas emissions from hydroelectric reservoirs in tropical regions. *Climatic Change*, 66(1–2), 9–21. <https://doi.org/10.1023/B:CLIM.0000043158.52222.ee>
- Rosa, L. P., dos Santos, M. A., Matvienko, B., Sikar, E., Lourenco, R. S. M., & Menezes, C. F. (2003). Biogenic gas production from major Amazon reservoirs, Brazil. *Hydrological Processes*, 17, 1443–1450.
- Soumis, N., Duchemin, E., Canuel, R., & Lucotte, M. (2004). Greenhouse gas emissions from reservoirs of the western United States. *Global Biogeochemical Cycles*, 18, GB3022. <https://doi.org/10.1029/2003GB002197>
- St. Louis, V. L., Kelly, C. A., Duchemin, E., Rudd, J. W. M., & Rosenberg, D. M. (2000). Reservoir surfaces as sources of greenhouse gases to the atmosphere: A global estimate. *Bioscience*, 50, 766–775. [https://doi.org/10.1641/0006-3568\(2000\)050\[0766:RSASOG\]2.0.CO;2](https://doi.org/10.1641/0006-3568(2000)050[0766:RSASOG]2.0.CO;2)
- Sturm, K., Yuan, Z., Gibbes, B., Werner, U., & Grinham, A. (2014). Methane and nitrous oxide sources and emissions in a subtropical freshwater reservoir, South East Queensland, Australia. *Biogeosciences*, 11(18), 5245–5258. <https://doi.org/10.5194/bg-11-5245-2014>
- Teodoru, C., Nyoni, F., Borges, A., Darchambeau, F., Nyambe, I., & Bouillon, S. (2015). Dynamics of greenhouse gases (CO₂, CH₄, N₂O) along the Zambezi River and major tributaries, and their importance in the riverine carbon budget. *Biogeosciences*, 12(8), 2431–2453.

- Teodoru, C. R., Bastien, J., Bonneville, M. C., Del Giorgio, P. A., Demarty, M., Garneau, M., et al. (2012). The net carbon footprint of a newly created boreal hydroelectric reservoir. *Global Biogeochemical Cycles*, 26, GB2016. <https://doi.org/10.1029/2011GB004187>
- Tremblay, A., Therrien, J., Hamlin, B., Wichmann, E., & LeDrew, L. J. (2005). *Greenhouse gas emissions—Fluxes and processes hydroelectric reservoirs and natural environments*. In Tremblay, A., Varfalvy, L., Roehm, C., & Garneau, M. (Eds.), (pp. 209–232). Springer.
- Wang, Y.-H., Huang, H.-H., Chu, C.-P., & Chuag, Y.-J. (2013). A preliminary survey of greenhouse gas emission from three reservoirs in Taiwan. *Sustainable Environment Research*, 23, 215–225.
- Wik, M., Varner, R. K., Walter Anthony, K., MacIntyre, S., & Bastviken, D. (2016). Climate-sensitive northern lakes and ponds are critical components of methane release. *Nature Geoscience*, 9, 99–105. <https://doi.org/10.1038/ngeo2578>
- Xiao, S. B., Wang, Y. C., Liu, D. F., Yang, Z., Lei, D., & Zhang, C. (2013). Diel and seasonal variation of methane and carbon dioxide fluxes at Site Guojiaba, the Three Gorges Reservoir. *Journal of Environmental Sciences*, 25, 2065–2071.
- Yang, L., Lu, F., Wang, X., Duan, X., Song, W., Sun, B., et al. (2013). Spatial and seasonal variability of diffusive methane emissions from the Three Gorges Reservoir. *Journal of Geophysical Research – Biogeosciences*, 118(2), 471–481. <https://doi.org/10.1002/jgrg.20049>
- Yang, M., Geng, X., Grace, J., Lu, C., Zhu, Y., Zhou, Y., & Lei, G. C. (2014). Spatial and seasonal CH₄ flux in the littoral zone of Miyun Reservoir near Beijing: The effects of water level and its fluctuation. *PLoS One*, 9, e94275.
- Zhao, Y., Wu, B. F., & Zeng, Y. (2013). Spatial and temporal patterns of greenhouse gas emissions from Three Gorges Reservoir of China. *Biogeosciences*, 10(2), 1219–1230. <https://doi.org/10.5194/bg-10-1219-2013>
- Zhen, F. (2012). *Greenhouse gas emission from Three Gorges Reservoir (upper Zhongxian County)*. China: Postdoctoral report in the University of Chinese Academy of Sciences.